https://doi.org/10.2352/ISSN.2169-4451.2017.32.446

Reprinted from
Journal of Imaging Science and Technology® 60(4): 040406-1–040406-6, 2016.

Growth-Inhibitory Effect of Chemotherapeutic Drugs Dispensed by Inkjet Bioprinting on Cancer and Non-Cancer Cells

Jorge I. Rodríguez-Dévora
Department of Metallurgical, Materials & Biomedical Engineering, University of Texas at El Paso, El Paso, Texas 79968, United States
Department of Bioengineering, Clemson University, Clemson, South Carolina 29634, United States
E-mail: jorger@clemson.edu

Mohammod Bhuyan, Daniel Reyna-Soriano, and Thomas Boland
Department of Metallurgical, Materials & Biomedical Engineering, University of Texas at El Paso, 500 W University Ave., El Paso, Texas 79968, United States

Abstract. *Thermal inkjet technology has long been used in the printing industry, but little has been studied on the benefits that it can provide to the drug-screening field. The objective of the work reported here was a proof of concept of using a modified inkjet printer to have a more accessible and miniature cellomic anticancer drug-screening platform. The authors' previous findings have shown that inkjet-based screening can reliably create isolated arrays of spots of living cells and antibiotics at low volume (180 pl) and high throughput (213 spots/sec) [J. I. Rodríguez-Dévora, B. Zhang, D. Reyna, Z. D. Shi, and T. Xu, "High throughput miniature drug-screening platform using bioprinting technology," Biofabrication* ***4****, 035001 (2012)]. The methodology of the work reported here included using a modified office inkjet printing device; the authors studied the inhibitory effects of dichloroacetate sodium (DCA) over hepatocellular carcinoma (HepG2) and epithelial cells (EpC). A DCA drug concentration gradient was printed over cell cultures to evaluate the drug's cytotoxic effect. Half maximal and ninety percent inhibitory concentrations (IC50, IC90) were obtained from the dose–response curves and compared with concentrations obtained using the traditional micropipetting technique. The resulting inhibitory concentration values obtained by both dispensing techniques fall within the millimolar range. The significance of these finding is that the proposed screening platform closely mimics the traditional screening outcome at a miniaturized volume rate, thus downsizing the screening process from traditional sub-microliter to nano- or even picoliter range. Inkjet technology shows promise in miniaturizing and expediting the drug-screening process. This platform can be used to asses a preliminary dose–response curve in order to improve the treatment modalities using the patient's limited supply of biopsied cells toward personalized medicine.* © *2016 Society for Imaging Science and Technology.*

INTRODUCTION

The new paradigm of personalized medicine is beginning to affect clinical practice. In particular, many of the advances in genomics and proteomics have made personalized screening and therapeutic inventions translate to the clinic.[1,2] Personalized medicine promises to refine diagnosis, guide optimum treatment, and avoid unnecessary side effects. In the envisioned personalized medicine protocol, analysis of a patient's own cells is required. In particular, biopsied cancer cells can be analyzed in vitro to screen them against potential therapeutic agents, thus defining the appropriate dose and treatment for the specific patient. To serve this purpose, the screening process has to develop in three phases: (a) assay methods and detection, (b) liquid handling and robotics, and (c) process flow and information management. The focus of this article relies on the development of the second phase. This phase is characterized by several requirements, including the capability of multiple cell dispensing, high throughput, effective utilization of reagents, and accuracy. Robotic systems based on extrusion technology had been set up as the standard process for the liquid handling phase.[3,4] In the desire to further miniaturize and expedite the screening process, the authors explored inkjet printing technology, which has shown promising results for fulfilling these requirements.[5] Inkjet technology has been explored for biological applications for close to a decade with positive results.[6–8] Efforts include, but are not limited to, the fabrication of high-throughput arrays,[9] tissue engineering constructs,[8,10–13] skin grafting,[14] stem cell differentiation,[15] and drug screening.[5,16]

Chemotherapy remains as a standard procedure for the treatment of most types of cancer. The "maximum tolerated dose" is used to ensure reduction in tumor volume and avoid recurrence; in practice, however, the dose intrinsically damages healthy cells of highly proliferating nature (i.e., intestinal epithelium, bone marrow, and hair follicles). To avoid these side effects, scientists search for new compounds possessing cytotoxic activity against cancer cells and mitigated or zero cytotoxicity to normal cells. The study reported here is a proof of concept on minimizing chemotherapy side effects by better relating the

Received Mar. 29, 2016; accepted for publication July 3, 2016; published online Aug. 2, 2016. Associate Editor: Rita Hofmann-Sievert.

most appropriate dosage to a particular tumor treatment (personalized medicine).

To minimize secondary effects of cancer treatment, normal cell lines associated with cancer cells must be screened. Epithelial, endothelial, and stem cells are ideal candidates for this purpose. Epithelial tissue lines and covers both organs and the whole body, and among the four main tissue types existing in the body (muscle, connective, nervous, and epithelial), the epithelial cells (EpCs) are the most abundant. This abundance makes EpCs more susceptible to being affected by cancer growth and anticancer treatments; therefore, EpCs are ideal for use as part of the screening to evaluate the expected side effects of any given anticancer drug regimen. The drug used in this study was dichloroacetate acid (DCA). DCA has been shown to reverse the glycolytic phenotype on numerous cancer cells by depolarizing the hyperpolarized inner mitochondrial membrane potential to normal levels and increasing mitochondrial metabolism.[17,18] Because DCA targets a change undergone during tumorigenesis, it has the potential to be effective against cancer cells without a toxic response to healthy cells. There is, however, an existing paradox due to contradictory results.[19]

Cell-based screening platforms are required to improve the assessment on clinical utility of large panels of novel chemotherapeutic compounds.[20] Monolayer cancerous cultures do not replicate the complexity of cancer. Development of technology is necessary to urge the parallel analysis of cellomic and genomic assays. Screening centers use commercially available dispensing units that can miniaturize the agents being screened; however, they represent a large investment. This creates an interest in exploring more accessible systems (i.e., inkjet technology) which can signify that more drug discovery activities will increase.

This article shows the use of a modified office printer which uses thermal inkjet technology as a potential contributor to create a better cell-based anticancer drug-screening process.

MATERIALS AND METHODS

Cell Lines and Culture Conditions

Human hepatocellular carcinoma (HepG2) and human prostate epithelial (EpC) cell lines were a gift from the laboratory of Dr. Jianying Zhang (Biology, UTEP). Both cell lines were cultured with Dulbecco's Modified Eagle's Medium (DMEM; Gibco BRL, Grand Island, NY, USA) supplemented with 10% fetal bovine serum and 1% penicillin/streptomycin in a humidified environment in 5% CO_2 at 37°C. In order to evaluate the selectivity of DCA, HepG2 and EpC were selected to evaluate the cytotoxic effect of DCA over cancerous and non-cancerous cell lines during the screening process.

Printing Suspensions and Printing Systems

Dichloroacetate acid (DCA) in the form of sodium dichloroacetate (AC33828, Fisher Scientific) was dissolved in dimethyl sulfoxide (DMSO) to a stock concentration

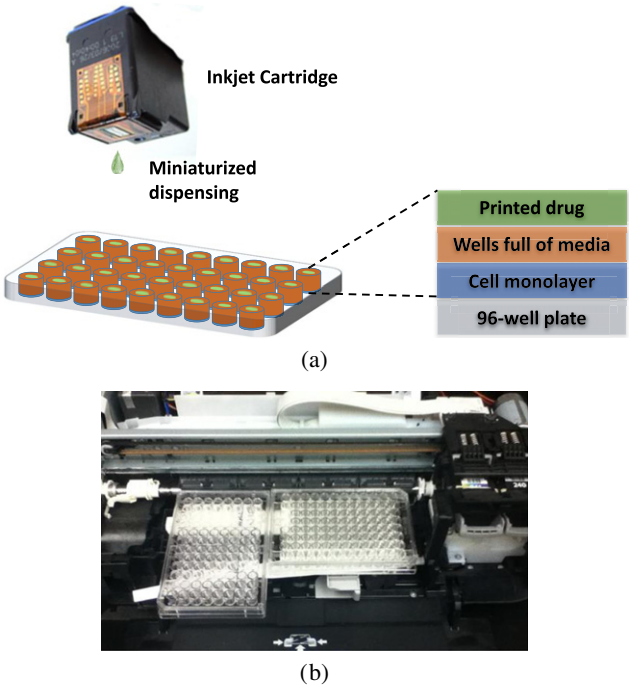

Figure 1. (a) Schematic illustration of the high-throughput inkjet printing platform dispensing drugs in a 96-well plate. (b) An actual image of the system accommodating two 96-well plates in different orientations.

of 10 mg/ml. This was further diluted by adding DMEM prior to adding the solution to the well containing the cell monolayer for a final concentration of less than 1% of DMSO. A wide range of concentrations in logarithmic increments (e.g., 1 μM–10 mM, and the no-drug control) were used for the first attempt; subsequently, a narrower range was used based on the results from the first range. Drug solutions were printed (dispensed) simultaneously using a modified thermal inkjet printing system (MG2120, Canon). This Canon system was characterized by nozzles that dispensed 1, 2, and 5 picoliters per activation time and speeds of 3.8 and 9.6 million droplets per second for black and color cartridges, respectively, based on estimated saturation throughput reported by Canon using the ISO/IEC 24734 standard.[21] Previous characterization of the volume dispensed by inkjet systems has been reported elsewhere.[5] The inkjet printing system was modified by overriding the paper-feeding sensors, removing the printing feeding mechanisms to allow printing over 96-well plates, and sterilizing cartridges and the nozzle-cleaning system. Figure 1(a) illustrates the printing platform, where drugs were dispensed on top of monolayer cultures. Fig. 1(b) shows how the modified system accommodates the 96-well plate in various orientations. One hundred microliters of drug stock solution was used to fill a sterilized cartridge (CL-241, Canon). In parallel, a traditional micropipette was used to run a cytotoxic assay in triplicate using microliter range solution.

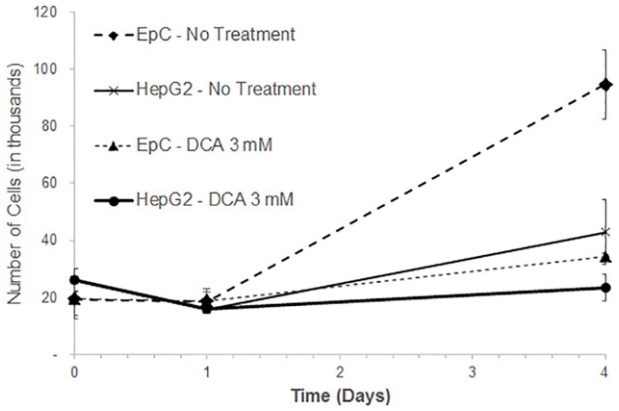

Figure 2. Proliferation of epithelial and hepatocellular cells at seeding time, day 0, and along drug exposure, day 1, under 3 mM DCA treatment and without treatment until the recovery period at day 4.

Drug-Screening Experimental Design

After passages 10–15, HepG2 and EpCs were trypsinized and counted using a hemocytometer (Countess® Automated Cell Counter, Invitrogen), and trypan blue staining was used to distinguish live cells prior to seeding. An optimization study was performed to ensure that cells were exposed to the drug while still in the exponential growth phase. Each experimental well was seeded with 20,000 ± 2500 cells. Drugs were added to cells after 24 hours in culture. Cell survival was evaluated via standard titration MTS cytotoxic assay, which measures the mitochondrial activity by formazan reduction. Colorimetric (MTS) assay was performed to determine the amount of viable cells upon 24 hours of drug exposure followed by 48 hours for cell recovery. In this last period, cells were allowed to proliferate for two to three population-doubling times (PDTs) to distinguish between cells that remained viable and were capable of proliferation and those that remained viable but could not proliferate. Figure 2 illustrates the proliferative behavior of mammalian cells with and without treatment. Different 96-well plates were used to compare the traditional method, micropipetting, with the investigated inkjet printing method. Half maximal and ninety percent inhibitory concentrations (IC50, IC90) were obtained from the dose–response curves. Assays were triplicated per drug concentration and no-drug control sample group. Drug concentrations were prepared between 1 and 50 mM for the micropipetting procedure, while a stock solution containing 10 mg/ml of each drug was used for the inkjet direct dispensing. The ejected volume was controlled by the inkjet printing system to print all samples in the same round, and to avoid the need for multiple subsets of drug concentrations. Drug control samples were defined as positive when stock drug concentration (high dosage) was used, and negative when DMSO was diluted in medium for a final concentration of less than 1% to ensure that the cytotoxic effect was due to the drug and not the presence of the DMSO.

Statistical Significance

Data were expressed as mean ± standard deviation (SD). Statistical significance was identified by Student's t-test. A p-value greater than 0.05 was considered to be statistically significant.

RESULTS AND DISCUSSION

Proliferation Studies for Seeding Stage

Following the MTS manufacturer's recommendation, the linear relationship between cell number and the absorbance values from the spectrophotometer was obtained for each cell type used in the drug-screening experiments. The plots show the linear relation between the MTS absorbance reading at 490 nm and the number of cells (data not reported). The slopes obtained were 27,146 and 37,683 cells/OD-value for EpCs and HepG2 cell lines, respectively. Higher concentrations were not considered as they did not fall under the linear phase,[22] which can result in misleading data. The end of the linear relation occurs when the number of cells is close to fully filling the culture surface, which was observed to be in the range of 60,000–80,000 cells per well for both cell lines. As result of this experiment, it was determined that optimal cell seeding was at 20,000 ± 2500 cells per well.

To determine the optimal time to introduce the drug treatment, proliferation assay was performed to determine the exponential growth curves of epithelial and HepG2 cell lines seeded at 20,000 cells per well. Samples were triplicated and MTS absorbance readings at 490 nm were obtained after 0, 24, 72, 120, 168, and 216 hours of culture. The ideal drug exposure period must start during the midline of the exponential growth. Thus, drug treatment was performed after the seeded cells had been in culture for 24 hours.

Inhibitory Effects

The survival fractions using the micropipette and inkjet techniques were obtained and are plotted in Figure 3. The dose–response curves show that the drug regimen had a similar effect on both cell lines. The drugs were dissolved in DMSO, as the literature indicates that it is more suitable for the screening process.[23,24] The resulting IC50 values were 2.46 and 3.10 mM for HepG2 and EpCs, respectively. The resulting IC90 values were 4.13 and 3.90 mM for HepG2 and EpCs, respectively. Fig. 3 shows the inhibitory effect of the drugs printed at varying concentrations. DCA showed small differences in IC50 between cell lines. Its IC50 values for EpCs and HepG2 were 1.89 and 2.05 mM, respectively. The resulting IC90s were 2.73 and 3.72 mM for HepG2 and EpCs, respectively.

Using a modified inkjet printer, anticancer drugs were arrayed on a 96-well plate to evaluate the inhibition of cancer growth under miniaturized volumes. The proposed platform was found to be comparable to the standard micropipetting-based screening process (p-value > 0.05), which suggests that the current standard process can be further miniaturized and expedited. Inkjet-based drug-screening results in a good candidate for screening extensive drug compounds and their combinations to better define the appropriate dose

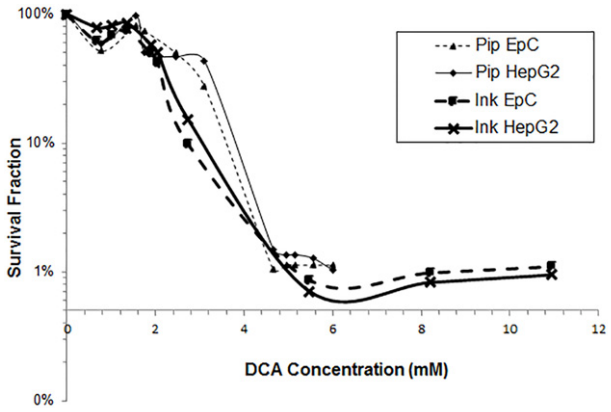

Figure 3. Dose–response curves by micropipetting and the proposed inkjet technique. Survival fraction of epithelial and HepG2 cell lines under (DCA) treatment at increasing concentrations when diluted in dimethyl sulfate oxide (DMSO). $n = 3$.

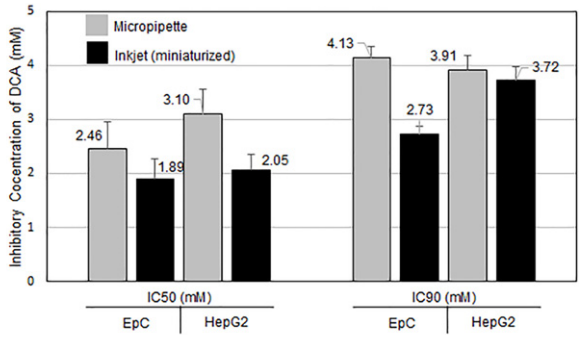

Figure 4. Histogram of identified half maximal and ninety percent inhibitory concentrations (IC50, IC90) for both techniques and cell lines.

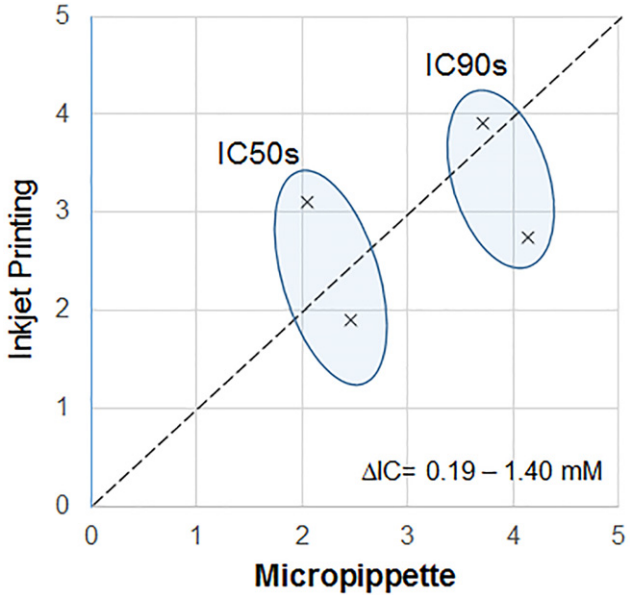

Figure 5. Correlation plot for half maximal inhibitory concentrations. This plot compares inkjet printing and manual micropipetting techniques.

for personalized medicine. This strategy shows potential for improving the accuracy of the treatment dose determination, deviating from the maximum tolerated dose, and, as a result, reducing the collateral damage to healthy proliferating cells. In the effort to achieve the promised benefits of personalized medicine, inkjet technology offers great potential. It can provide information to the oncologist prior to defining the chemotherapeutic treatment, and ultimately increases the chances of treatment success.

To date, it has been difficult to generalize the efficacy of DCA against all kinds of cancerous tumors. While positive responses from DCA against in vitro tumors have been reported at clinically relevant concentrations of 0.5–1 mM,[17,18,25,26] others have not shown cytotoxicity on particular cell lineages or mutations.[27–29] Thus, the basis for the limited anticancer effect of DCA in culture is likely to lie in the complex cellular physiology and the excess of metabolites present in culture media.[19]

The half maximal inhibitory coefficients from both screening techniques, micropipetting and inkjet-based, varied by less than 2 mM. In the resulting inhibition coefficients it can be observed that micropipetting required a slightly higher dose, which can be explained by the inherent variations of the two dispensing systems. It has been recognized[22,30] that the IC90 provides a more reliable dose that can effectively inhibit a given virus, bacteria, or disease model. Moreover, it has been identified that when using MTS, it is difficult to obtain reliable data at the IC90 or greater.[30] This explains the increased differences in IC90 values across technologies. Thus, future studies will benefit from using a more sensitive cytotoxic assay (i.e., ATP assay). Figure 4 is a histogram of the IC50 and IC90 values, where the resulting coefficients were significantly similar between traditional screening and the proposed inkjet method ($p < 0.05$).

The ideal chemotherapeutic drug candidate is expected to not have a cytotoxic effect over healthy tissues/cells. Unfortunately, the drugs in this study did not show selectivity toward cancerous cell lines, as shown in the dose–response curves in Fig. 3. This confirms the previously published cytotoxicity of DCA[27–29] over healthy cell lines.

Inhibitory Concentrations Across Technologies

Fig. 4 shows a summary of the inhibitory concentrations obtained. It can be observed that the inhibitory concentration at 50 and 90 percent are statistically and significantly similar across technologies (Student's t-test, $p > 0.05$). When comparing with literature reports, Sun et al.[31] reported that around 5 mM of DCA is sufficient to inhibit 50% of cell proliferation. Moreover, Figure 5 shows a direct correlation plot between inkjet-based and micropipetted IC50 and IC90 values. These results indicate that inkjet printing has the potential to minimize screening processes and result in similar outcomes to those elicited by higher-volume assays. A review of standard screening technologies is accessible elsewhere.[32]

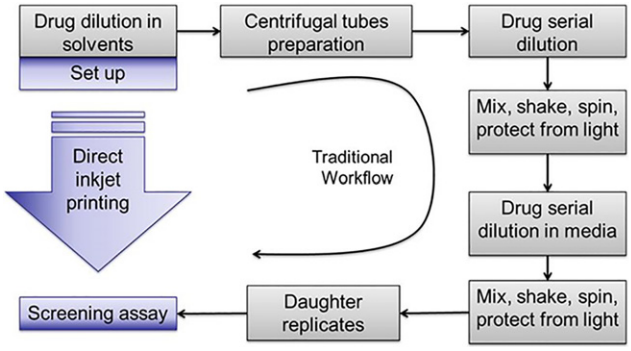

Figure 6. Schematic comparing the traditional workflow for the drug-screening process and the proposed direct inkjet printing platform.

Screening Process Optimization

The traditional screening process consists of many steps for the preparation of drugs, including drug dilution in solvents for stock concentration, preparation of centrifugal tubes, drug serial dilution for desired concentration, secondary dilution of the culturing medium, later duplicating, triplicating, or quadruplicating samples, and remembering that throughout the whole process, it is necessary to maintain homogeneous suspensions to avoid precipitations. While robotic systems have been designed to help with this biological task, there are many disadvantages, such as accumulated pipetting error, carryover, edge effects, excessive use of disposable materials (tips, centrifugal tubes), and relatively high volume consumption (in the range of microliters). In order to solve these issues, inkjet printing systems have emerged to reduce the preparation time of drug concentrations. Drug stock concentrations can be loaded into the inkjet-headed cartridge, and the precise volume control dispenses the replicates, creating immediate blends to expedite the screening process. A set-up time is initially required when implementing direct inkjet printing, but can be used for further trials. Figure 6 illustrates the optimization process.

CONCLUSIONS

The results obtained show that both cell lines were growth inhibited under a DCA chemotherapeutic regimen. The IC50 and IC90 values obtained by micropipetting and inkjet-based screening were significantly similar, suggesting that the proposed screening platform closely mimics the traditional screening outcome. The resulting IC50 and IC90 values indicate that 1.89 and 2.05 mM will be sufficient to inhibit growth of both cell lines under DCA treatment, respectively. In comparison to the literature, the IC50 results vary based on the cell lines used for the screening platform, but are generally in the range of 0.5–1 mM. Therefore, our results are consistent with ones that use much larger volumes, validating that the proposed inkjet-based screening assays can be further miniaturized.

Inkjet technology shows promise for use in determining dosages and treatment modalities using a patient's limited supply of biopsied cells. Future studies of the screening process using other drugs and biopsied cells from cancer patients will result in valuable data to foresee the efficiency of potential drug therapies. In its transition toward a clinical setting, the fabrication of three-dimensional functionalized microtissues is expected to better mimic the behavior of targeted tissues in vivo.

ACKNOWLEDGMENT

The authors would like to thank NIH—National Heart, Lung, and Blood Institute (NHLBI) (grant #1SC2HL107235-01), National Science Foundation (grant#CBET0936238), Department of Education (grant #P116V090013) for funding this project, and the department of scholarships of the Secretary of Education in Chihuahua, Mexico for their support. Special thanks are also due to Ms. Emily Gyemant and Ms. Jenny Bourne for serving as a resource on the English language.

REFERENCES

[1] G. S. Ginsburg and J. J. McCarthy, "Personalized medicine: revolutionizing drug discovery and patient care," Trends Biotechnol. **19**, 491–496 (2001).
[2] A. D. Weston and L. Hood, "Systems biology, proteomics, and the future of health care: toward predictive, preventative, and personalized medicine," J. Proteome Res. **3**, 179–196 (2004).
[3] J. L. Coffman, J. F. Kramarczyk, and B. D. Kelley, "High-throughput screening of chromatographic separations: I. Method development and column modeling," Biotechnol. Bioeng. **100**, 605–618 (2008).
[4] W. Y. Yeong, C. K. Chua, K. F. Leong, and M. Chandrasekaran, "Rapid prototyping in tissue engineering: challenges and potential," Trends Biotechnol. **22**, 643–652 (2004).
[5] J. I. Rodríguez-Dévora, B. Zhang, D. Reyna, Z. D. Shi, and T. Xu, "High throughput miniature drug-screening platform using bioprinting technology," Biofabrication **4**, 035001 (2012).
[6] M. Nakamura, A. Kobayashi, F. Takagi, A. Watanabe, Y. Hiruma, K. Ohuchi, Y. Iwasaki, M. Horie, I. Morita, and S. Takatani, "Biocompatible inkjet printing technique for designed seeding of individual living cells," Tissue Eng. **11**, 1658–1666 (2005).
[7] T. Boland, T. Xu, B. Damon, and X. Cui, "Application of inkjet printing to tissue engineering," Biotechnol. J. **1**, 910–917 (2006).
[8] M. Nakamura, Y. Nishiyama, C. Henmi, K. Yamaguchi, S. Mochizuki, T. Koki, and H. Nakagawa, "Inkjet bioprinting as an effective tool for tissue fabrication," *Proc. IS&T Digital Fabrication 2006* (IS&T, Springfield, VA, 2006), pp. 89–92.
[9] E. A. Roth, T. Xu, M. Das, C. Gregory, J. J. Hickman, and T. Boland, "Inkjet printing for high-throughput cell patterning," Biomaterials **25**, 3707–3715 (2004).
[10] T. Xu, J. Jin, C. Gregory, J. J. Hickman, and T. Boland, "Inkjet printing of viable mammalian cells," Biomaterials **26**, 93–99 (2005).
[11] R. E. Saunders, J. E. Gough, and B. Derby, "Delivery of human fibroblast cells by piezoelectric drop-on-demand inkjet printing," Biomaterials **29**, 193–203 (2008).
[12] D. Reyna, J. I. Rodriguez-Devora, M. Bhuyan, and T. Boland, "Inkjet bioprinting of solid peroxide microparticles for constructing oxygen-generating scaffolds," *Proc. IS&T NIP29: 29th Int'l. Conf. on Digital Printing Technologies and Digital Fabrication 2013* (IS&T, Springfield, VA, 2013), pp. 240–243.
[13] E. Hoch, A. Weber, and K. Borchers, "Biopolymer-based functional inks for the preparation of artificial cartilage via bioprinting technology," *Proc. IS&T NIP31: 31st Int'l. Conf. on Digital Printing technology and Digital Fabrication 2015* (IS&T, Springfield, VA, 2015), pp. 397–401.
[14] M. Yanez, J. Rincon, P. Cortez, N. Guenther, T. Boland, and C. D. Maria, "Printable cellular scaffold using self-crosslinking agents," J. Imaging Sci. Technol. **56**, 40506 (2012).

[15] S. Ilkhanizadeh, A. I. Teixeira, and O. Hermanson, "Inkjet printing of macromolecules on hydrogels to steer neural stem cell differentiation," Biomaterials **28**, 3936–3943 (2007).
[16] G. Arrabito and B. Pignataro, "Inkjet printing methodologies for drug screening," Anal. Chem. **82**, 3104–3107 (2010).
[17] J. Y. Wong, G. S. Huggins, M. Debidda, N. C. Munshi, and I. De Vivo, "Dichloroacetate induces apoptosis in endometrial cancer cells," Gynecol. Oncol. **109**, 394–402 (2008).
[18] S. Bonnet, S. L. Archer, J. Allalunis-Turner, A. Haromy, C. Beaulieu, R. Thompson, C. T. Lee, G. D. Lopaschuk, L. Puttagunta, G. Harry, K. Hashimoto, C. J. Porter, M. A. Andrade, B. Thebaud, and E. D. Michelakis, "A mitochondria-K+ channel axis is suppressed in cancer and its normalization promotes apoptosis and inhibits cancer growth," Cancer Cells **11**, 37–51 (2007).
[19] I. Papandreou, T. Goliasova, and N. C. Denko, "Anticancer drugs that target metabolism: is dichloroacetate the new paradigm?," Int. J. Cancer **128**, 1001–1008 (2011).
[20] S. Sharma, C. Santiskulvong, L. A. Bentolila, J. Rao, O. Dorigo, and J. K. Gimzewski, "Correlative nanomechanical profiling with super-resolution F-actin imaging reveals novel insights into mechanisms of cisplatin resistance in ovarian cancer cells," Nanomedicine **8**, 757–766 (2012).
[21] Canon inc, Adaption of ISO Productivity Standards. https://www.usa.canon.com/internet/portal/us/home/products/groups/iso-productivity-standards (accessed 3/23/2016).
[22] I. Freshney, "Culture of animal cells. A manual of basic technique," *A Manual of Basic Technique and Specialized Applications*. 6th ed. (Wiley-Blackwell, 2010) 365–380. http://www.wiley.com/WileyCDA/WileyTitle/productCd-0470528125.html .
[23] K. V. Balakin, N. P. Savchuk, and I. V. Tetko, "In silico approaches to prediction of aqueous and DMSO solubility of drug-like compounds: trends, problems and solutions," Curr. Med. Chem. **13**, 223–241 (2006).
[24] C. A. Lipinski, F. Lombardo, B. W. Dominy, and P. J. Feeney, "Experimental and computational approaches to estimate solubility and permeability in drug discovery and development settings," Adv. Drug. Deliv. Rev. **46**, 3–26 (2001).
[25] K. M. Anderson, J. Jajeh, P. Guinan, and M. Rubenstein, "In vitro effects of dichloroacetate and CO2 on hypoxic HeLa cells," Anticancer Res. **29**, 4579–4588 (2009).
[26] W. Cao, S. Yacoub, K. T. Shiverick, K. Namiki, Y. Sakai, S. Porvasnik, C. Urbanek, and C. J. Rosser, "Dichloroacetate (DCA) sensitizes both wild-type and over expressing Bcl-2 prostate cancer cells in vitro to radiation," Prostate **68**, 1223–1231 (2008).
[27] W. Sun, S. Zhou, S. S. Chang, T. McFate, A. Verma, and J. A. Califano, "Mitochondrial mutations contribute to HIF1alpha accumulation via increased reactive oxygen species and up-regulated pyruvate dehydrogenase kinase 2 in head and neck squamous cell carcinoma," Clin. Cancer Res. **15**, 476–484 (2009).
[28] L. H. Stockwin, S. X. Yu, S. Borgel, C. Hancock, T. L. Wolfe, L. R. Phillips, M. G. Hollingshead, and D. L. Newton, "Sodium dichloroacetate selectively targets cells with defects in the mitochondrial ETC," Int. J. Cancer **127**, 2510–2519 (2010).
[29] D. Heshe, S. Hoogestraat, C. Brauckmann, U. Karst, J. Boos, and C. Lanvers-Kaminsky, "Dichloroacetate metabolically targeted therapy defeats cytotoxicity of standard anticancer drugs," Cancer Chemother Pharmacol. **67**, 647–655 (2011).
[30] Y. Kano, M. Akutsu, S. Tsunoda, H. Mano, Y. Sato, Y. Honma, and Y. Furukawa, "In vitro cytotoxic effects of a tyrosine kinase inhibitor STI571 in combination with commonly used antileukemic agents," Blood **97**, 1999–2007 (2001).
[31] R. C. Sun, M. Fadia, J. E. Dahlstrom, C. R. Parish, P. G. Board, and A. C. Blackburn, "Reversal of the glycolytic phenotype by dichloroacetate inhibits metastatic breast cancer cell growth in vitro and in vivo," Breast Cancer Res. Treat **120**, 253–260 (2010).
[32] L. Mattheakis, "Screening robotics and automation," J. Biomolecular Screening **20**, 299–301 (2015).